Supporting Information

2D Boron Dichalcogenides from the Substitution of Mo with Ionic B_2 Pair in MoX_2(X = S, Se and Te): High Stability, Large Excitonic Effect and High Charge Carrier Mobility

Cheng Tang[1], Fengxian Ma[2], Chunmei Zhang[1], Yalong Jiao[1], Sri Kasi Matta[1], Ken Ostrikov[1] and Aijun Du[1,]*

[1]School of Chemistry, Physics and Mechanical Engineering, Queensland University of Technology, Gardens Point Campus, QLD 4001, Brisbane, Australia

[2]Department of Physics, Hebei Normal University, Shijiazhuang 050024, PR China

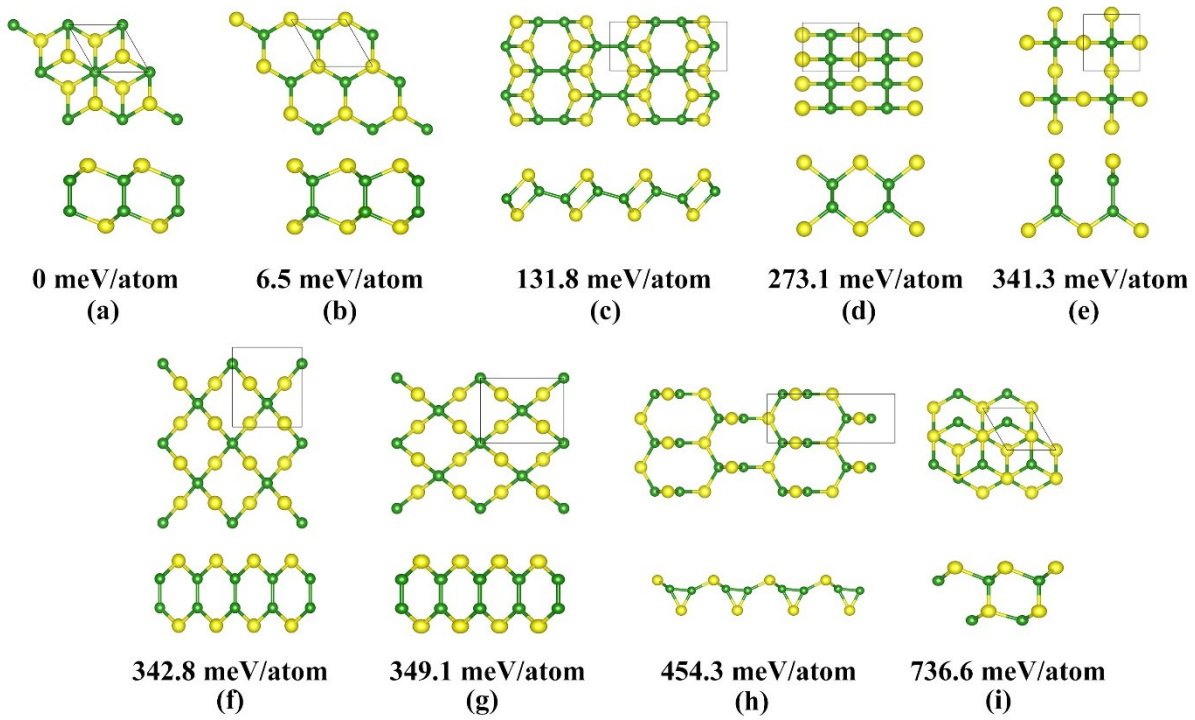

Figure S1. $(B_2S_2)_x$ (x = 1 and 2) monolayers with lower energy searched by the CALYPSO code. The relative energies with respect to the lowest one are calculated by PBE functional. The yellow and green balls represent sulphur and boron atoms, respectively. The black frames are boundaries of primitive cells.

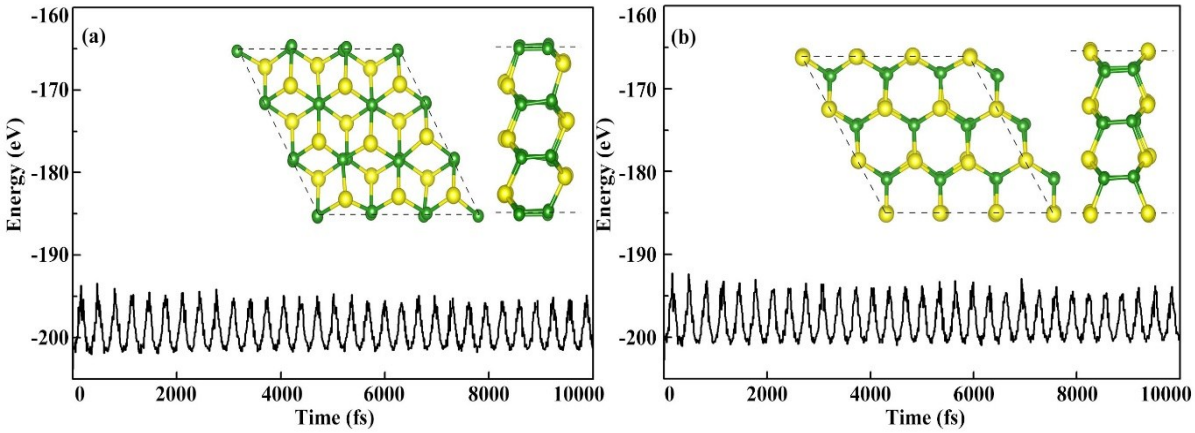

Figure S2. Total potential energies of (a) T- and (b) H-B_2S_2 fluctuate during the AIMD simulation at 1000 K. The top and side views of B_2S_2 at the end of AIMD simulation (10 ps) are inserted in the pictures, respectively. The yellow and green balls represent sulphur and boron atoms, respectively.

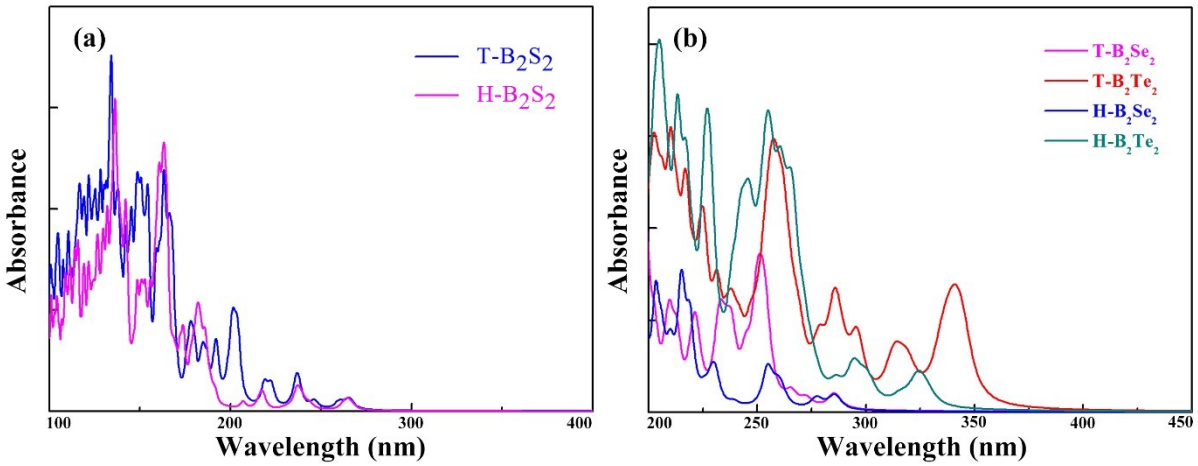

Figure S3. Light absorbance spectra for (a) B_2S_2 and (b) B_2Se_2 and B_2Te_2 monolayers calculated by HSE functional.

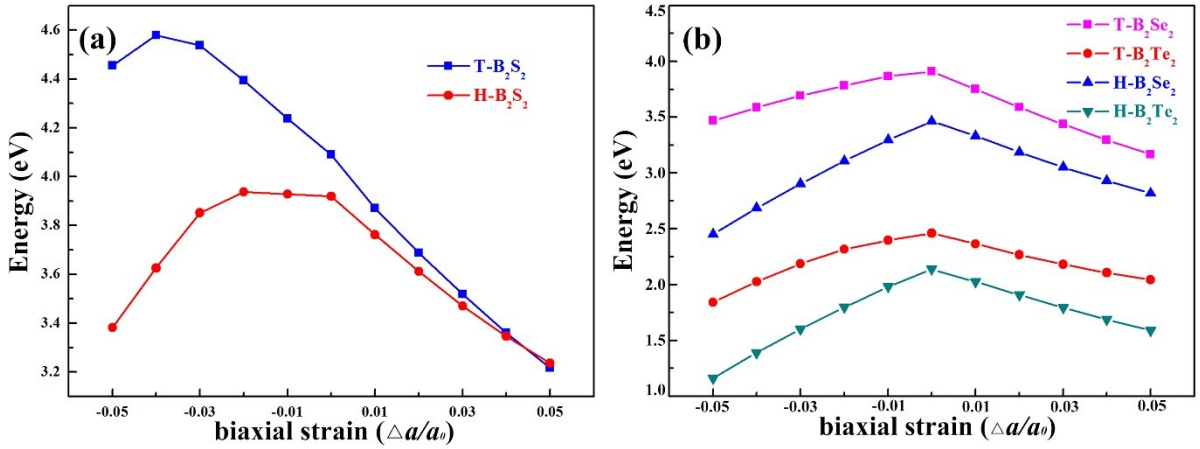

Figure S4. (a) Bandgaps as a function of biaxial strain obtained for T- (blue line) and H-B_2S_2 (red line) monolayers. (b) Bandgaps for T-B_2Se_2 (pink line), H-B_2Se_2 (blue line), T-B_2Te_2 (red line) and H-B_2Te_2 (dark green line) monolayers. All the results are calculated by HSE functional.

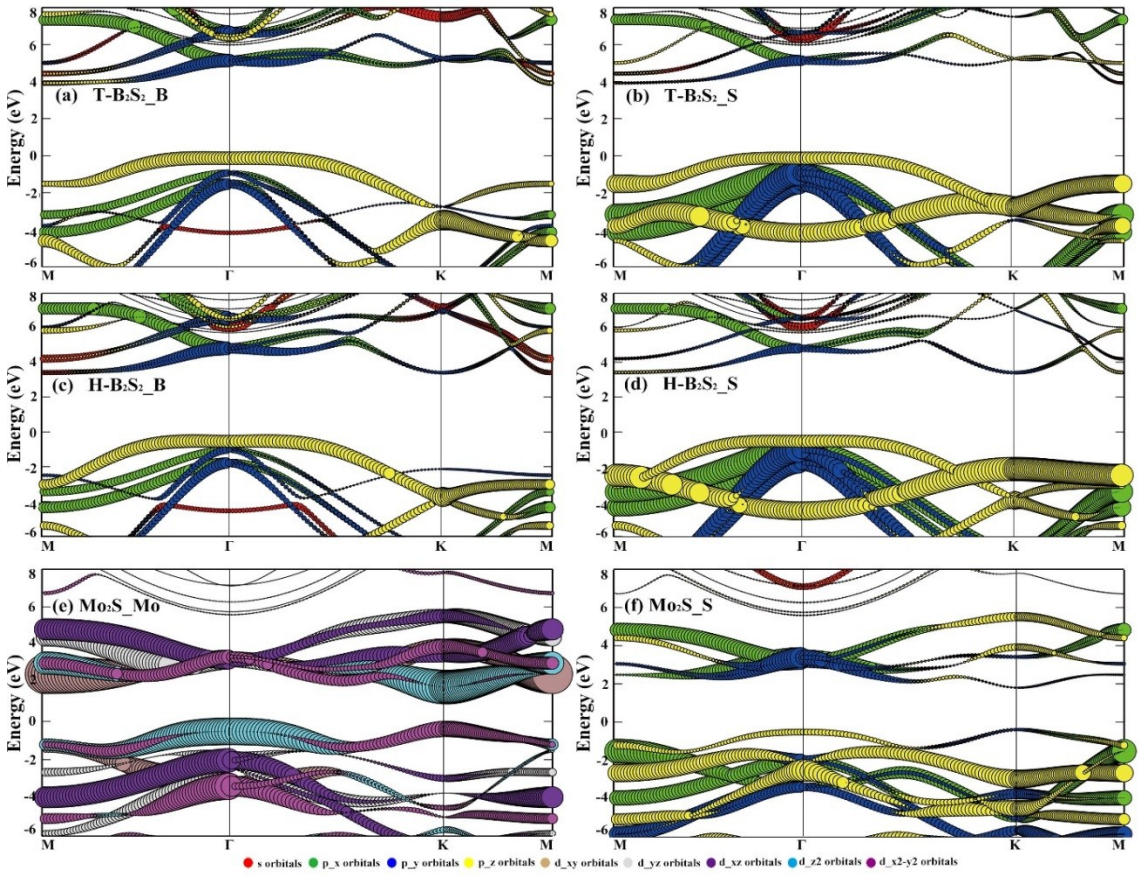

Figure S5. Orbital-resolved band structures of (a, b) T-B_2S_2, (c, d) H-B_2S_2, (e, f) H-MoS_2. The colourful circles represent different orbitals, which are shown at the bottom of the figure (red for s orbitals, green for p_x orbitals, blue for p_y orbitals, yellow for p_z orbitals, brown for d_{xy} orbitals, grey for d_{yz} orbitals, violet for d_{xz} orbitals, cyan for d_z^2 orbitals, and magenta for $d_{x^2-y^2}$ orbitals). Fermi level has been set to zero.

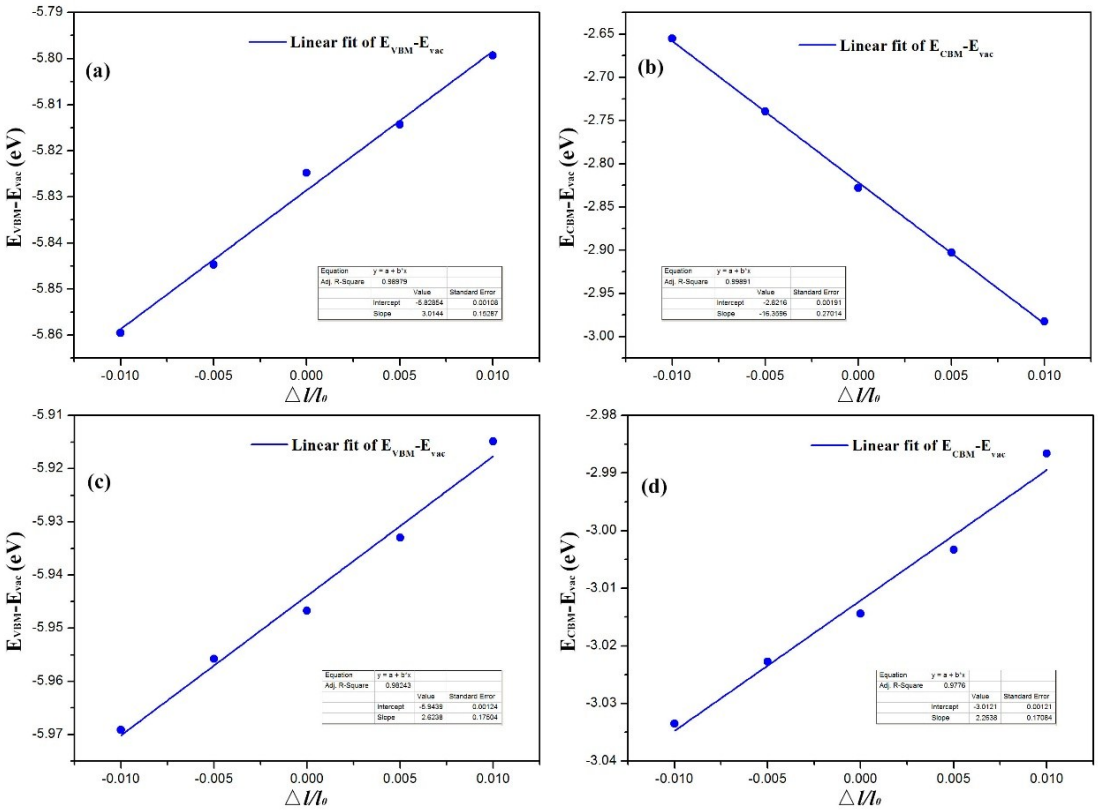

Figure S6. Linear fitting of deformation potential for T-B_2S_2 (a, b) and H-B_2S_2 (c, d), respectively. The PBE functional was used to calculate the deformation potential for reducing the computational cost.

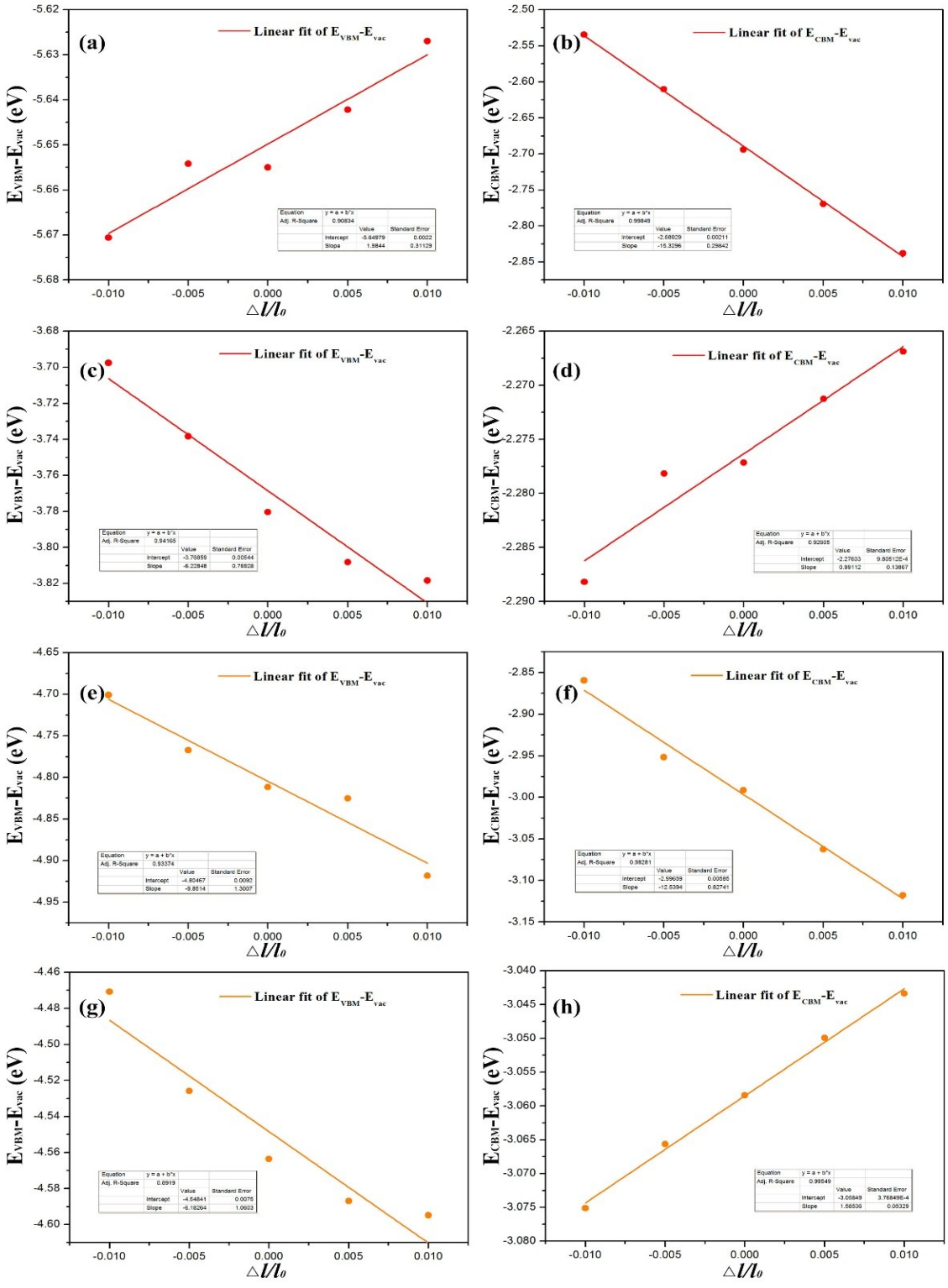

Figure S7. Linear fitting of deformation potential for T-B_2Se_2 (a, b), H-B_2Se_2 (c, d), T-B_2Te_2 (e, f), and H-B_2Te_2 (g, h), respectively. The PBE functional was used to calculate the deformation potential for reducing the huge computational cost.

Table S1. Relative effective mass (m^*), elastic modulus (C_{2D}), and deformation potential (E_l^i) for T- and H-B_2X_2, respectively. The symbol $m^*_{M\text{-}\Gamma}$ indicates the relative effective mass along the M-Γ direction, and the rest can be defined in the same manner. For hole mobility, since the VBM of B_2S_2 and T-B_2Se_2 locate between Γ and K point, $m^*_{V\text{-}K}$ represents the relative effective mass along Γ-K direction (from VBM to K point), on the contrary, $m^*_{V\text{-}\Gamma}$ represent that from VBM to Γ point.

Carrier type		Relative effective mass (m^*/m_0)				C_{2D} (J/m^2)	E_l (eV)
		$m^*_{M\text{-}\Gamma}$	$m^*_{M\text{-}K}$	$m^*_{K\text{-}\Gamma}$	$m^*_{K\text{-}M}$		
electron	T-B_2S_2	2.159	0.033	---	---	236.852	-16.360
	H-B_2S_2	---	---	0.094	0.088	249.469	2.264
	T-B_2Se_2	1.227	0.027	---	---	189.636	-15.330
	H-B_2Se_2	---	---	0.085	0.084	206.195	0.991
	T-B_2Te_2	0.453	0.026	---	---	147.872	-12.539
	H-B_2Te_2	---	---	0.074	0.072	159.218	1.585
		$m^*_{V\text{-}K}$		$m^*_{V\text{-}\Gamma}$			
hole	T-B_2S_2	0.784		1.435		236.852	3.014
	H-B_2S_2	0.673		1.092		249.469	2.624
	T-B_2Se_2	0.291		0.435		189.636	1.984
		$m^*_{\Gamma\text{-}M}$		$m^*_{\Gamma\text{-}K}$			
	H-B_2Se_2	0.101		0.099		206.195	-6.228
	T-B_2Te_2	0.089		0.087		147.872	-9.851
	H-B_2Te_2	0.067		0.067		159.218	-6.183

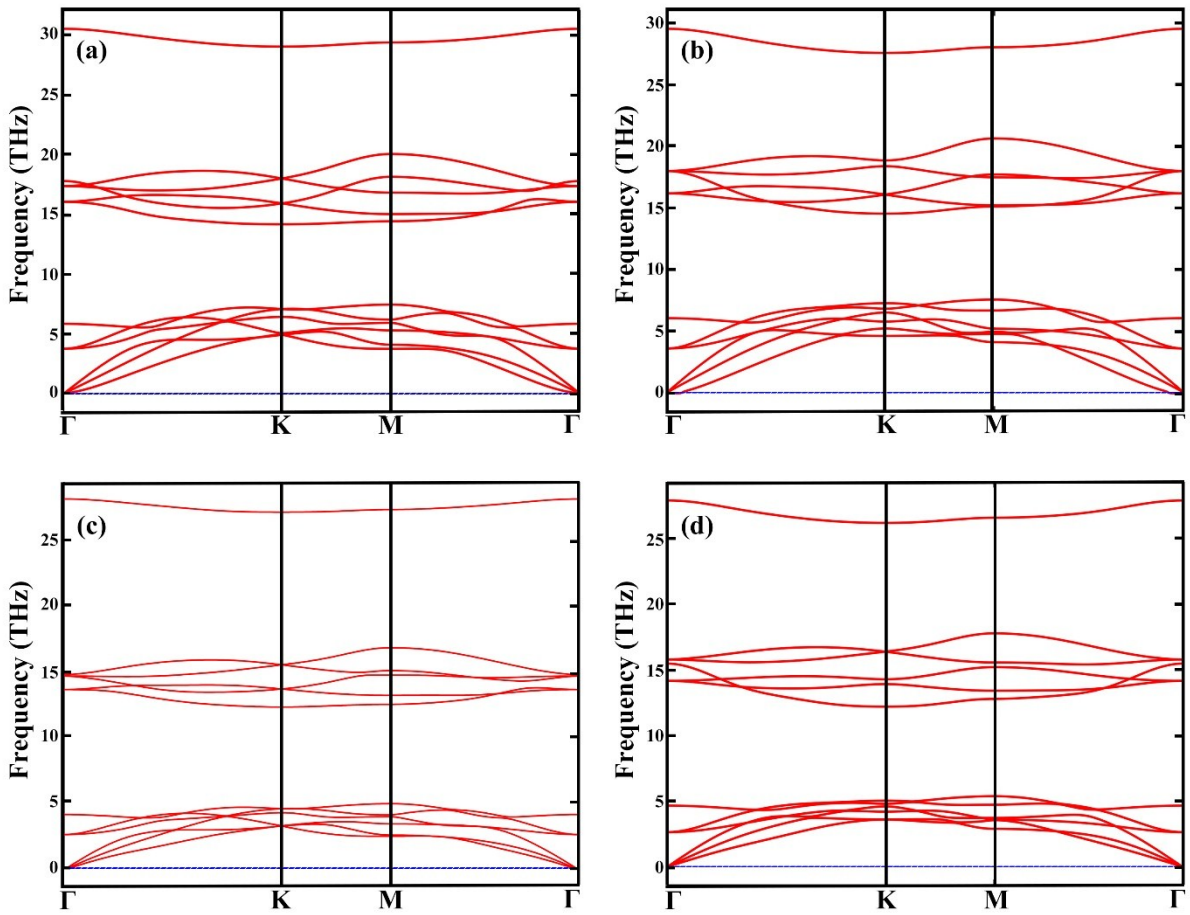

Figure S8. Phonon spectra of (a) T- and (b) H-B_2Se_2, (c) T- and (d) H-B_2Te_2 monolayers.

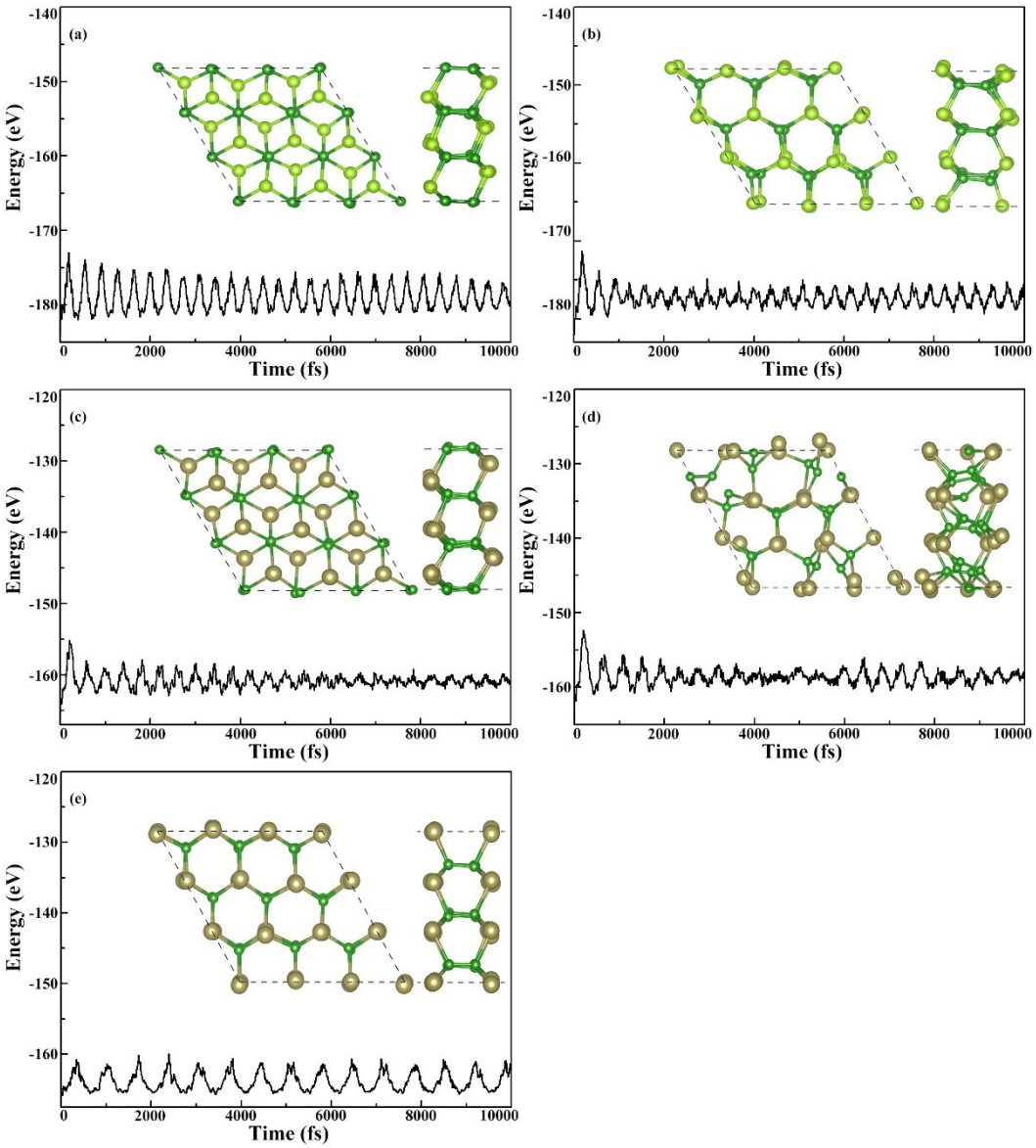

Figure S9. Total potential energies of (a) T-B_2Se_2, (b) H-B_2Se_2 (c) T-B_2Te_2, and (e) T-B_2Te_2 fluctuate during the AIMD simulation at 1000 K. The top and side views of B_2S_2 at the end of AIMD simulation (10 ps) are inserted in the pictures, respectively. (e) Total potential energies of T-B_2Te_2 at 300 K. Green, light green, and brown balls represent boron, selenium, and tellurium atoms, respectively.

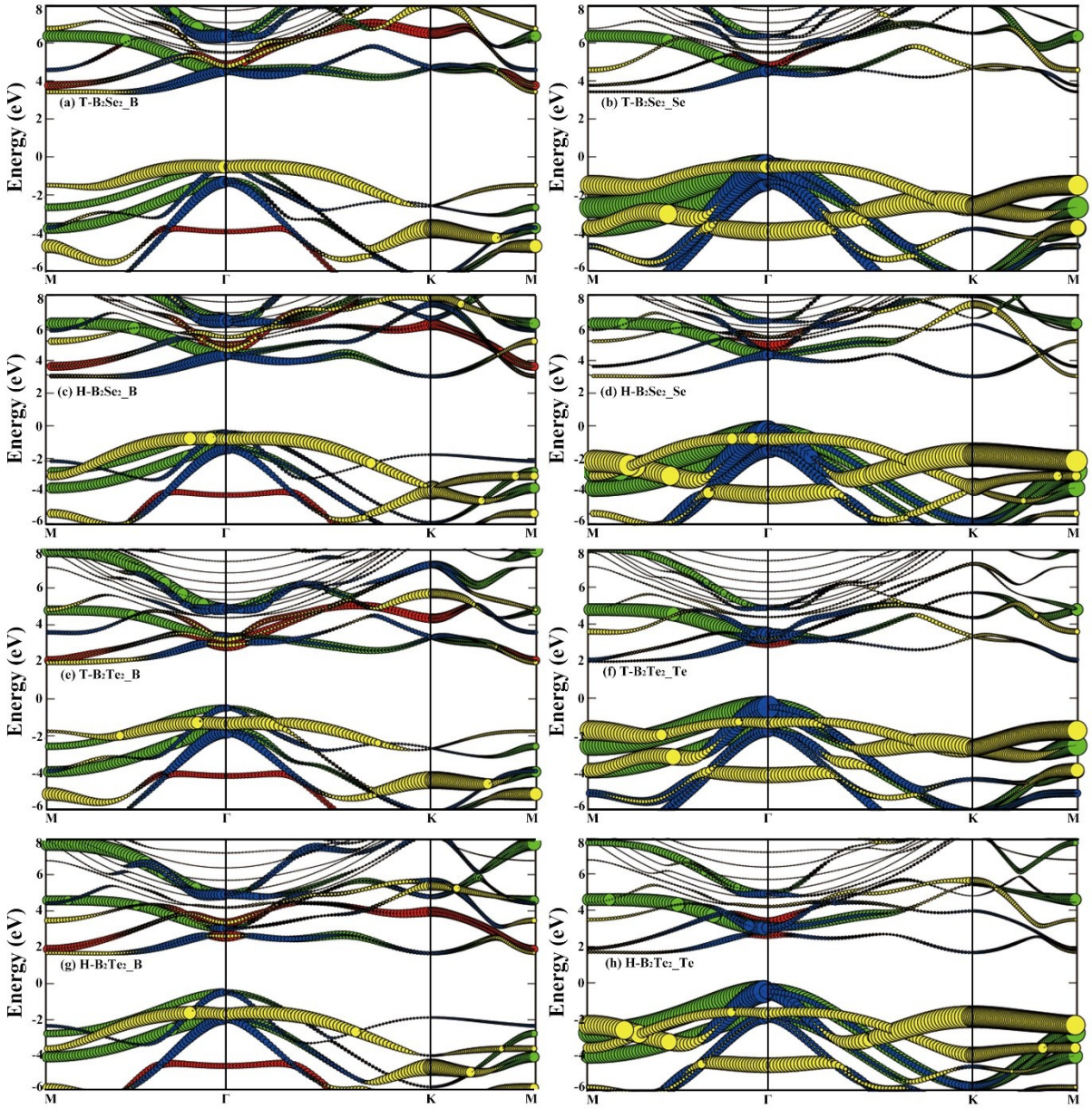

Figure S10. Orbital-resolved band structures of (a, b) T-B_2Se_2, (c, d) H-B_2Se_2, (e, f) T-B_2Te_2 and (g, h) H-B_2Te_2. The colourful circles has the same meaning of Fig. S2. Fermi level has been set to zero.

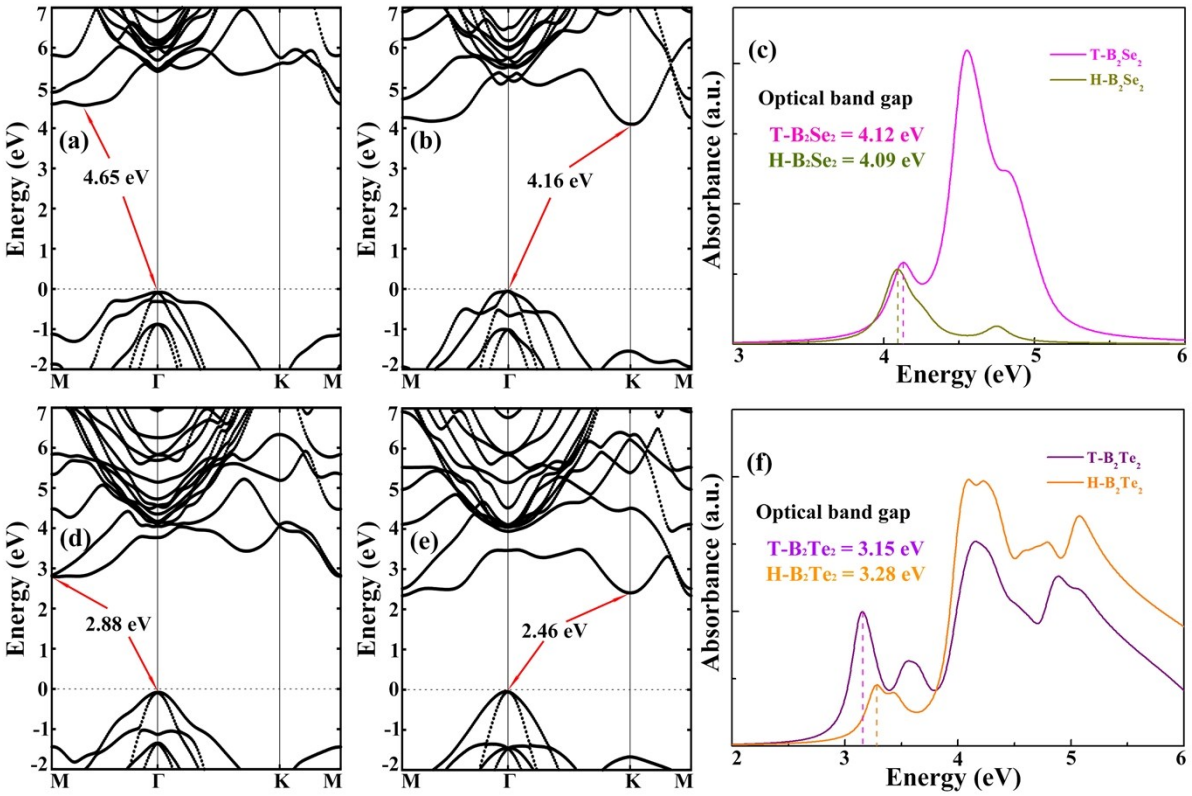

Figure S11. *GW* band structures of (a) T-B_2Se_2, (b) H-B_2Se_2, (d) T-B_2Te_2, and (e) H-B_2Te_2. Fermi levels are set to zero. BSE-optical absorption spectrum of (c) B_2Se_2 and (f) B_2Te_2 monolayers. Based on the *GW* band structures, the direct bandgaps of T-B_2Se_2, H-B_2Se_2, T-B_2Te_2 and H-B_2Te_2 are 5.06 eV, 4.94 eV, 3.85 eV, and 3.51 eV, respectively.